Chemical Science

ROYAL SOCIETY OF CHEMISTRY

EDGE ARTICLE

View Article Online
View Journal | View Issue

Cite this: *Chem. Sci.*, 2024, **15**, 6891

All publication charges for this article have been paid for by the Royal Society of Chemistry

Received 4th February 2024
Accepted 12th March 2024

DOI: 10.1039/d4sc00836g

rsc.li/chemical-science

$HgBr_2$: an easily growing wide-spectrum birefringent crystal†

Ming-Shu Zhang,[ac] Wen-Dong Yao,[d] Shao-Min Pei,[a] Bin-Wen Liu, *[ab] Xiao-Ming Jiang [ab] and Guo-Cong Guo *[ab]

Birefringent materials are of great significance to the development of modern optical technology; however, research on halide birefringent crystals with a wide transparent range remains limited. In this work, mercuric bromide ($HgBr_2$) has been investigated for the first time as a promising birefringent material with a wide transparent window spanning from ultraviolet (UV) to far-infrared (far-IR) spectral regions (0.34–22.9 μm). $HgBr_2$ has an exceptionally large birefringence (Δn, 0.235 @ 546 nm), which is 19.6 times that of commercial MgF_2. The ordered linear motif [Br–Hg–Br] with high polarizability anisotropy within the molecule is the inherent source of excellent birefringence, making it an efficient building block for birefringent materials. In addition, $HgBr_2$ can be easily grown under mild conditions and remain stable in air for prolonged periods. Studying the birefringent properties of $HgBr_2$ crystals would provide new ideas for future exploration of wide-spectrum birefringent materials.

Introduction

Birefringence is manifested by the existence of orientation-dependent differences in the refractive index, which is widely used in the fields of optical polarization, optical modulation, and nonlinear optics.[1–7] The exploration of birefringent materials is an essential topic in the field of optical research.[8–15] To date, a diverse range of oxide and halide birefringent materials with high chemical stability have garnered significant interest, including MgF_2,[16] α-BaB_2O_4,[17] YVO_4,[18] TiO_2,[19] $LiNbO_3$,[20] $CaCO_3$,[21] *etc.* However, the aforementioned birefringent materials are plagued by various inherent defects: MgF_2 possesses a tiny birefringence; α-BaB_2O_4 encounters issues such as phase transition and cracking during growth; TiO_2 demonstrates high hardness and poses challenges in terms of processing; YVO_4 cannot be utilized within the ultraviolet band; $LiNbO_3$ exhibits a low laser-induced damage threshold and is susceptible to photorefractive damage; $CaCO_3$ is deliquescent and difficult to obtain high-quality single crystals. Hence, it holds immense significance for practical applications to discover birefringent materials with substantial birefringence, multi-wave applicability, excellent chemical and physical stability, as well as favorable crystal growth habits.

Metal halides are highly regarded as important optical function materials due to their advantages of easy preparation, rich coordination environment, wide transparent range, high laser-induced damage threshold, and are applied in the frontier fields of luminescence, solar cells, laser frequency conversion, and so on.[22–29] Among them, binary metal halides are widely utilized owing to their simple composition and cost-effectiveness: KBr is commonly employed as a background material in Fourier transform infrared (FT-IR) spectroscopy due to its wide transparent range exceeding 25 μm;[30] CaF_2 and BaF_2 exhibit excellent mechanical properties, thermal stability, and radiation resistance along with high transparency from deep ultraviolet (UV) to IR regions, which are applied in optical prisms, lenses, wedge plates, diaphragms and other important optical components.[31] By reason of the foregoing, the splendid physical and chemical properties of binary metal halides are in line with our expectations for the next generation of birefringent crystal materials, making them regarded as a treasury of birefringent materials with great potential. On the other hand, metal halides display diverse coordination patterns, including linear, trigonal pyramidal, tetrahedral, and square pyramidal structures, which offer promising opportunities for identifying building blocks with significant polarizability anisotropy for birefringent materials.[25] Through comparison and screening, binary mercury-based (Hg-based) halides have emerged as a focal point for us due to their abundant configurations and broad transparent range. In Hg-based halides, apart from the traditional $[HgX_4]$ (X = halogen) tetrahedra, there also exist infrequent [X–Hg–X] or [X–Hg–Hg–X] linear units.[32–36] In

[a]*State Key Laboratory of Structural Chemistry, Fujian Institute of Research on the Structure of Matter, Chinese Academy of Sciences, Fuzhou, Fujian 350002, P. R. China*
[b]*Fujian Science & Technology Innovation Laboratory for Optoelectronic Information of China, Fuzhou, Fujian 350108, P. R. China*
[c]*University of Chinese Academy of Sciences, Beijing 100049, P. R. China*
[d]*School of Chemistry and Chemical Engineering, Yangzhou University, Yangzhou, Jiangsu 225002, P. R. China*

† Electronic supplementary information (ESI) available: Experimental section, crystallographic data, EDS and PXRD patterns of $HgBr_2$. See DOI: https://doi.org/10.1039/d4sc00836g

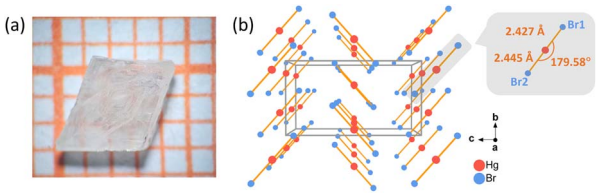

Fig. 1 (a) The single-crystal $HgBr_2$ with a size of 4 × 3 × 2 mm^3; (b) the structure of $HgBr_2$ viewed along the *a*-axis (left) and the coordination environment of the Hg atom (right).

borates, the linear unit [BO_2] is thought to have greater polarizability anisotropy than the classic [BO_3],[37,38] and the previous studies of HgB_2S_4 and trigonal HgS have suggested that the [S–Hg–S] linear units have strong birefringent contributions (0.28 at 1064 nm and 0.29 at 2100 nm, respectively).[39,40] Moreover, the [X–Hg–Hg–X] motif in the binary mercurous halide can induce a giant birefringence; however, prolonged exposure to light can lead to decomposition of mercurous halide.[41] Therefore, the linear [X–Hg–X] unit can also be regarded as a potential emerging building block of birefringent materials; however, its comprehensive investigation remains insufficient. Moreover, binary mercuric halides offer greater advantages in terms of synthesis and crystal growth, with their growth conditions generally being more moderate, thereby facilitating the achievement of large-scale crystal growth and device fabrication. Consequently, simple halides composed of linear [X–Hg–X] units are promising birefringent materials. In this work, mercuric bromide was selected as a potential birefringent material for the first time. A colorless single-crystal of mercuric bromide with a size of 4 × 3 × 2 mm^3 was successfully obtained through a slow solvent evaporation technique employing hot ethanol as the solvent (as shown in Fig. 1a). The birefringence of $HgBr_2$ at 546 nm is 0.235, which is 19.6 times higher than that of another commercial binary halide material, MgF_2 (0.012 @ 546 nm).[16] Moreover, $HgBr_2$ demonstrates a transparent range spanning from 0.34 to 25 μm, effectively covering an ultrawide transparent range from UV to far-IR. The rationality of the experimental results is confirmed by theoretical calculations, indicating the potential of mercuric bromide as a next-generation birefringent material.

Results and discussion

We have computationally determined the polarizability anisotropy and HOMO–LUMO gap of five Hg-based linear units (three [HgX_2], X = Cl, Br, I; two [HgQ_2], Q = S, Se), aiming to substantiate their potential as birefringent materials and analyze their respective merits and demerits. As depicted in Fig. 2a, the polarizability anisotropy of most Hg-based linear units is comparable to or even surpasses that of [BS_3], the novel IR birefringent material building unit. Among them, [HgX_2] exhibits a wider HOMO–LUMO gap compared to [BS_3], which is advantageous for achieving a wider band gap and a higher laser-induced damage threshold for meeting the application requirements of materials in high-energy laser systems. For instance, previous studies have demonstrated that the laser-induced damage threshold of $HgBr_2$ reaches 0.3 GW cm^{-2},[35] significantly surpassing those of the [BS_3]-based compounds, such as $Ca_2La(BS_3)(SiS_4)$ (34.43 MW cm^{-2}), $LaBS_3$ (49.55 MW cm^{-2}) and BaB_2S_4 (265 MW cm^{-2}).[42–44] Although the polarization anisotropy of [HgQ_2] is 1.7 to 2 times that of [BS_3], their HOMO–LUMO gap is narrower, which would affect their optical band gap. For the above-mentioned reason, the [HgX_2] units are potential building units with comparable performance to [BS_3], suggesting that Hg-based binary halides composed of [HgX_2] may serve as possible wide-spectrum birefringent materials. Considering the hydrolysis susceptibility of $HgCl_2$ and the narrow band gap exhibited by HgI_2, we selected $HgBr_2$ as our subject for investigating birefringence properties.

The crystal growth procedure of $HgBr_2$ is as follows: a saturated solution of mercury bromide was prepared in a beaker using hot anhydrous ethanol as the solvent under continuous agitation. Subsequently, the clear solution was filtered while still hot into another beaker, and the solvent was very slowly evaporated at room temperature. After one month, a substantial quantity of crystals with two to four millimeter-sized were successfully acquired. The analytical results based on the crystallographic data obtained by single-crystal XRD demonstrate that $HgBr_2$ crystal crystallizes in the orthorhombic space group $Cmc2_1$, and the cell parameters are: a = 4.6215(6) Å, b = 6.7794(7) Å, c = 12.4277(19) Å, and Z = 4, which are consistent with the results reported in previous literature.[43] The structure of $HgBr_2$ is a simple zero-dimensional (0D) arrangement consisting of isolated [$HgBr_2$] units (Fig. 1b), with one crystallographically independent Hg atom and two Br atoms in each asymmetric unit. The bond lengths of Hg–Br range from 2.427(6) Å to 2.445(7) Å, and the angle of ∠Br–Hg–Br is 179.58°, both of which align with the corresponding values documented in the literature.[45] In general, the majority of three-dimensional (3D) structural frameworks constructed from metal-centered coordination tetrahedra typically exhibit low anisotropy and small birefringence, whereas lower-dimensional structures tend to display significant anisotropy and consequently induce appreciable birefringence.[46] Therefore, the combination of the 0D structure of $HgBr_2$ and the 1D linear building unit [$HgBr_2$] with a large polarizability anisotropy will facilitate the generation of large birefringence.

The optical band gap of $HgBr_2$ gained by UV-vis-NIR diffuse-reflectance spectroscopy processed by the Tauc plot method was 3.60 eV (Fig. 2c),[47] which was slightly higher than the band gap reported in previous literature (3.3 eV),[35] larger than those of some commercial IR optical materials such as $AgGaS_2$ (2.76 eV), $AgGaSe_2$ (1.83 eV),[48] ZnSe (2.58 eV) and comparable to that of ZnS (3.72 eV).[49,50] The wider optical band gap can effectively mitigate the damage caused by photon absorption to the material, thereby enhancing the laser-induced damage threshold for application in high-energy laser systems. In addition, according to the diffuse reflection spectrum, the UV cutoff edge of $HgBr_2$ was about 344 nm. Combined with the IR spectrum, it can be determined that the transparent range of $HgBr_2$ was 0.34–22.9 μm (Fig. 2c), covering a broad spectral range from UV to far-IR, surpassing those of all commercially

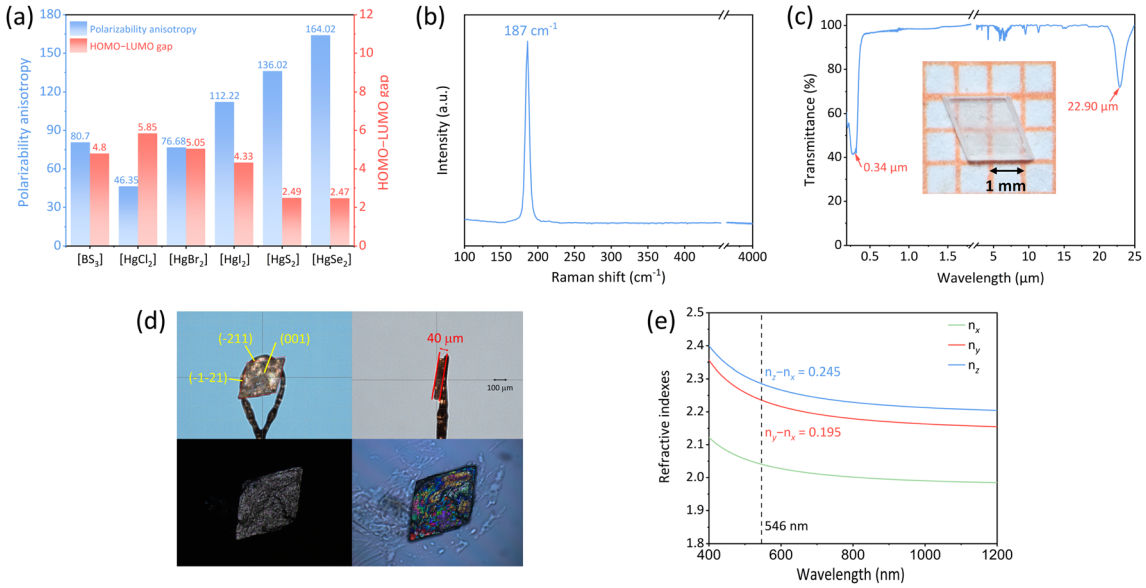

Fig. 2 (a) Polarizability anisotropy and HOMO–LUMO gaps of the [BS_3], [$HgCl_2$], [$HgBr_2$], [HgI_2], [HgS_2], and [$HgSe_2$] units; (b) experimental Raman spectrum of $HgBr_2$; (c) UV-vis-IR transmittance spectrum collected from the single crystal (inside: the photograph of single crystal $HgBr_2$ plate); (d) crystallographic orientation and birefringence measurement of the $HgBr_2$ crystal; (e) the calculated birefringence values of $HgBr_2$.

available birefringent materials. The wide transparency range of $HgBr_2$ can be attributed to two aspects: the substantial atomic weight of mercury and bromine atoms leads to their low phonon energy thus enabling high transmittance in the far-IR region; additionally, the high electronegativity of bromine leads to a strong bond of valence electrons, consequently yielding a broad optical band gap. In addition, the sharp absorption peak at 4.2 μm in Fig. 2c originates from the asymmetric stretching vibration of the C=O double bond in carbon dioxide molecules; the dense and sharp absorption peaks observed within the range of 5–8 μm may be attributed to the bending vibrations of hydroxyl groups in gaseous water molecules; the two minor absorption peaks detected at wavelengths of 9.5 μm and 11.3 μm can be ascribed to stretching and bending vibrations associated with C–O single bonds present in ethanol molecules. Given our utilization of ethanol as a solvent for crystal growth purposes, it is possible for weak IR absorption features related to ethanol to emerge within the IR spectrum. The Raman spectrum of $HgBr_2$ is shown in Fig. 2b. The peak at 187 cm^{-1} has roots in the vibration of the Hg–Br bond,[51] and no other peaks are found in the range from 4000 to 100 cm^{-1}.

To thoroughly investigate the potential of $HgBr_2$ as a birefringent material, crystal $HgBr_2$ was measured using a polarizing microscope equipped with a 546 nm light source. The crystal of $HgBr_2$ chosen for the birefringence test is depicted in Fig. 2d. The crystallographic plane of the single crystal for birefringence measurement was confirmed as (001) through orientation using single-crystal XRD. Referring to the Michel-Levy Birefringence Chart, the optical path difference of the measured crystal was 9411.707 nm, and its thickness was 0.04 mm, and thus a calculated value of 0.235 can be assigned to the refractive index difference of this crystal under 546 nm illumination, which surpassed that of commercially available birefringent material MgF_2 (0.012)[16] and even those of recently reported binary halides $SbCl_3$ (0.172) and α-SnF_2 (0.177) containing stereochemical activity lone pairs.[52] Since $HgBr_2$ crystallized in the orthorhombic system and belonged to a biaxial crystal, there were three refractive indices (n_x, n_y, and n_z) along the *x*-, *y*-, and *z*-axes, respectively. The relationship between these refractive indices was given as $n_z > n_y > n_x$. The maximum birefringence of $HgBr_2$ occurred at the (010) crystallographic plane, which corresponded to the difference between n_z and n_x. However, due to the intrinsic growth habit of $HgBr_2$, it was challenging to expose the (010) plane effectively. Despite attempts to mechanically cut the crystal to obtain an exposed (010) plane, we have been unsuccessful in producing a wafer that met the testing conditions of a polarizing microscope. Therefore, considering that the measured crystal plane of $HgBr_2$ was not parallel to the optical axis plane, the birefringence obtained at the (001) crystal plane should be less than or equal to $n_z - n_x$ and close to $n_y - n_x$. As presented in Fig. 2e, the maximum calculated refractive index difference ($n_z - n_x$) of $HgBr_2$ was 0.245 at 546 nm and the value of $n_y - n_x$ was 0.195, which exhibited good agreement with the experimental birefringence measurement and our conjecture. Despite challenges associated with exposing specific crystallographic planes in the $HgBr_2$ crystal for accurate measurement purposes, our findings demonstrate that there is still agreement between theoretical calculations and experimental results when it comes to understanding its birefringent properties on other crystal planes, which has not received enough attention in previous similar studies.

We have conducted a statistical analysis for classical birefringent materials (MgF_2, α-BaB_2O_4, YVO_4, TiO_2, $LiNbO_3$, $CaCO_3$),[16–21] recently reported birefringent materials with large

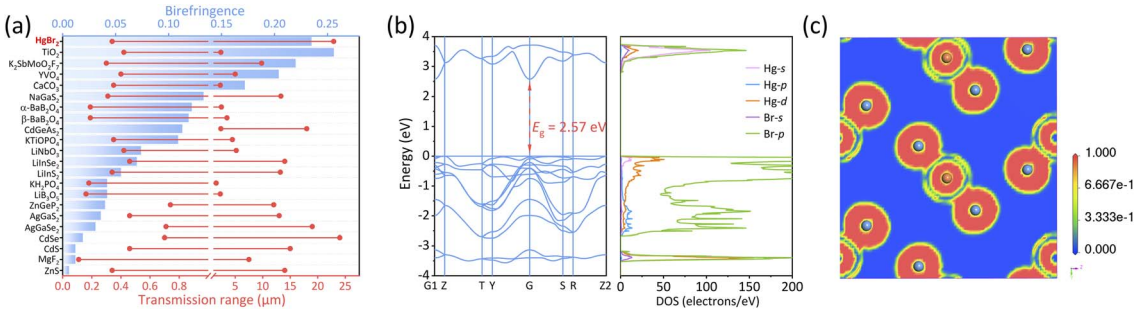

Fig. 3 (a) Comparison of $HgBr_2$ with typical optical crystals in terms of birefringence and transmission range; (b) the calculated band structure (left) and density of states (DOS, right) of $HgBr_2$; (c) 2D ELF diagram through the [Br–Hg–Br] motif for $HgBr_2$.

crystals ($K_2SbMoO_2F_7$, $NaGaS_2$),[46,53] common commercial nonlinear optical materials (LiB_3O_5, β-BaB_2O_4, KH_2PO_4, $KTiOPO_4$, $AgGaS_2$, $AgGaSe_2$, $ZnGeP_2$, $CdGeAs_2$),[48] and some chalcogenide optical materials (ZnS, CdS, CdSe)[54–56] to compare them with $HgBr_2$ in terms of transparent range and birefringence. Note that the transparent spectra of these materials were tested based on large crystals, ensuring high reliability. Additionally, most of the refractive index tests for these materials were performed using an ~550 nm light source, except for narrow band gap materials including $AgGaSe_2$ (@2000 nm), CdSe (@2000 nm), $ZnGeP_2$ (@2000 nm) and $CdGeAs_2$ (@3000 nm). From Fig. 3a, it is evident that $HgBr_2$ ranked among the top in both the spectral transparent range and birefringence among these optical materials; specifically, $HgBr_2$ possessed a transparent range that exceeds those of most birefringent materials, and its birefringent performance is second only to TiO_2 among commercial birefringent materials, which demonstrated that $HgBr_2$ has great potential as a wide-spectrum birefringent material.

In order to better understand the relationship between the structure and properties, the electronic structure of $HgBr_2$ has been calculated based on the first-principles method. As depicted in Fig. 3b (left), $HgBr_2$ was a direct bandgap semiconductor with a calculated band gap of 2.57 eV, which slightly deviates from the experimental optical band gap (3.60 eV) due to the inherent limitation of the GGA-PBE functional caused by the discontinuity of exchange correlation energy, resulting in an underestimation of the band gap.[57] However, this value is consistent with the previous calculation by Kanchana *et al.* without using the TB-mBJ functional (2.24 eV).[58] The DOS of $HgBr_2$ is shown in Fig. 3b (right). The top of the valence band (VB) and the bottom of the conduction band (CB) were mainly governed by Hg-6s, Hg-5d, and Br-4p orbitals, indicating that the optical properties of $HgBr_2$ were predominantly influenced by [$HgBr_2$] units. The electron localization function (ELF) maps projected on crystal planes parallel to [$HgBr_2$] motifs were further subjected to analysis. As illustrated in Fig. 3c, the electron cloud around the [$HgBr_2$] motif exhibited a dumbbell-like shape and demonstrates large optical anisotropy, which was the primary cause of the significant birefringence in $HgBr_2$. The above results further validated the rationality of the experimental findings.

Conclusions

In summary, we have investigated $HgBr_2$ as a wide-spectrum birefringent material for the first time and successfully obtained a large number of millimeter-scale single crystals through simple and mild growth methods. The findings revealed that $HgBr_2$ possessed a broad band gap (3.60 eV) and transparent range (0.34–22.9 μm), and notably, it displayed a large birefringence that is 19.6 times that of the commercial halide MgF_2, thereby demonstrating $HgBr_2$ as a promising wide-spectrum birefringent material. Furthermore, we substantiated for the first time *via* theoretical calculations that the Hg-based linear unit possessed a significant polarizability anisotropy, qualifying it as a potential candidate for constructing superior birefringent materials. This work will provide a novel idea for the design and exploration of wide-spectrum birefringent materials in the future.

Data availability

Data available on request from the authors.

Author contributions

Ming-Shu Zhang: conceptualization, data curation, visualization, writing – original draft; Wen-Dong Yao: theoretical calculations; Shao-Min Pei: data curation, theoretical calculations; Bin-Wen Liu: writing – review & editing; Xiao-Ming Jiang: software; Guo-Cong Guo: supervision.

Conflicts of interest

There are no conflicts to declare.

Acknowledgements

This work was supported by the National Natural Science Foundation of China (21827813, 21921001, 22175172, 22075283, 92161125, and U21A20508), the Youth Innovation Promotion Association of Chinese Academy of Sciences (2020303 and 2021300), and Fujian Science & Technology Innovation Laboratory for Optoelectronic Information of China (grant no. 2020ZZ108).

Notes and references

1 M. Mutailipu, J. Han, Z. Li, F. M. Li, J. J. Li, F. F. Zhang, X. F. Long, Z. H. Yang and S. L. Pan, Achieving the Full-Wavelength Phase-Matching for Efficient Nonlinear Optical Frequency Conversion in $C(NH_2)_3BF_4$, *Nat. Photonics*, 2023, **17**, 694–701.

2 S. Y. Niu, G. Joe, H. Zhao, Y. C. Zhou, T. Orvis, H. X. Huyan, J. Salman, K. Mahalingam, B. Urwin, J. B. Wu, Y. Liu, T. E. Tiwald, S. B. Cronin, B. M. Howe, M. Mecklenburg, R. Haiges, D. J. Singh, H. Wang, M. A. Kats and J. Ravichandran, Giant Optical Anisotropy in A Quasi-One-Dimensional Crystal, *Nat. Photonics*, 2018, **12**, 392–396.

3 F. Y. Xu, X. W. L. Chen, M. Q. Zhang, L. Y. Wang, R. Y. Wei and Q. P. Wang, Study on Birefringent Crystal Beamsplitter, *Proc. SPIE*, 1995, **2540**, 182–189.

4 A. Tagaya, H. Ohkita, M. Mukoh, R. Sakaguchi and Y. Koike, Compensation of the Birefringence of a Polymer by a Birefringent Crystal, *Science*, 2003, **301**, 812–814.

5 Z. Y. Xie, L. G. Sun, G. Z. Han and Z. Z. Gu, Optical Switching of a Birefringent Photonic Crystal, *Adv. Mater.*, 2008, **20**, 3601–3604.

6 R. Appel, C. D. Dyer and J. N. Lockwood, Design of a broadband UV-visible α-barium borate polarizer, *Appl. Opt.*, 2002, **41**, 2470–2480.

7 M. Koga and T. Matsrnmoto, High-Isolation Polarization-Insensitive Optical Circulator for Advanced Optical Communication Systems, *J. Lightwave Technol.*, 1992, **10**, 1210–1217.

8 M. Zhang, D. H. An, C. Hu, X. L. Chen, Z. H. Yang and S. L. Pan, Rational Design *via* Synergistic Combination Leads to an Outstanding Deep-Ultraviolet Birefringent $Li_2Na_2B_2O_5$ Material with an Unvalued B_2O_5 Functional Gene, *J. Am. Chem. Soc.*, 2019, **141**, 3258–3264.

9 Y. Yang, Y. Qiu, P. F. Gong, L. Kang, G. M. Song, X. M. Liu, J. L. Sun and Z. S. Lin, Lone-Pair Enhanced Birefringence in an Alkaline-Earth Metal Tin(II) Phosphate $BaSn_2(PO_4)_2$, *Chem.–Eur. J.*, 2019, **25**, 5648–5651.

10 N. Z. Wang, F. Liang, Y. Yang, S. Z. Zhang and Z. S. Lin, A New Ultraviolet Transparent Hydra-Cyanurate $K_2(C_3N_3O_3H)$ with Strong Optical Anisotropy from Delocalized π-Bonds, *Dalton Trans.*, 2019, **48**, 2271–2274.

11 Y. C. Liu, X. M. Liu, S. Liu, Q. R. Ding, Y. Q. Li, L. N. Li, S. G. Zhao, Z. S. Lin, J. H. Luo and M. C. Hong, An Unprecedented Antimony(III) Borate with Strong Linear and Nonlinear Optical Responses, *Angew. Chem., Int. Ed.*, 2020, **59**, 7793–7796.

12 J. Y. Guo, A. Tudi, S. J. Han, Z. H. Yang and S. L. Pan, $Sn_2B_5O_9Cl$: A Material with Large Birefringence Enhancement Activated Prepared *via* Alkaline-Earth-Metal Substitution by Tin, *Angew. Chem., Int. Ed.*, 2019, **58**, 17675–17678.

13 X. L. Chen, B. B. Zhang, F. F. Zhang, Y. Wang, M. Zhang, Z. H. Yang, K. R. Poeppelmeier and S. L. Pan, Designing an Excellent Deep-Ultraviolet Birefringent Material for Light Polarization, *J. Am. Chem. Soc.*, 2018, **140**, 16311–16319.

14 C. C. Jin, F. M. Li, B. L. Cheng, H. T. Qiu, Z. H. Yang, S. L. Pan and M. Mutailipu, Double-Modification Oriented Design of a Deep-UV Birefringent Crystal Functionalized by $[B_{12}O_{16}F_4(OH)_4]$ Clusters, *Angew. Chem., Int. Ed.*, 2022, **61**, e202203984.

15 C. C. Jin, X. P. Shi, H. Zeng, S. J. Han, Z. Chen, Z. H. Yang, M. Mutailipu and S. L. Pan, Hydroxyfluorooxoborate $Na[B_3O_3F_2(OH)_2][B(OH)_3]$: Optimizing the Optical Anisotropy with Heteroanionic Units for Deep Ultraviolet Birefringent Crystals, *Angew. Chem., Int. Ed.*, 2021, **60**, 20469.

16 M. J. Dodge, Refractive Properties of Magnesium Fluoride, *Appl. Opt.*, 1984, **23**, 1980–1985.

17 G. Q. Zhou, J. Xu, X. D. Chen, H. Y. Zhong, S. T. Wang, K. Xu, P. Z. Deng and F. X. Gan, Growth and Spectrum of a Novel Birefringent α-BaB_2O_4 Crystal, *J. Cryst. Growth*, 1998, **191**, 517–519.

18 H. T. Luo, T. Tkaczyk, E. L. Dereniak, K. Oka and R. Sampson, High Birefringence of the Yttrium Vanadate Crystal in the Middle Wavelength Infrared, *Opt. Lett.*, 2006, **31**, 616–618.

19 J. R. DeVore, Refractive Indices of Rutile and Sphalerite, *J. Opt. Soc. Am.*, 1951, **41**, 416–419.

20 D. E. Zelmon, D. L. Small and D. Jundt, Infrared Corrected Sellmeier Coefficients for Congruently Grown Lithium Niobate and 5 mol.% Magnesium Oxide-Doped Lithium Niobate, *J. Opt. Soc. Am. B*, 1997, **14**, 3319–3322.

21 G. Ghosh, Dispersion-Equation Coefficients for the Refractive Index and Birefringence of Calcite and Quartz Crystals, *Opt. Commun.*, 1999, **163**, 95–102.

22 M. Z. Li and Z. G. Xia, Recent Progress of Zero-Dimensional Luminescent Metal Halides, *Chem. Soc. Rev.*, 2021, **50**, 2626–2662.

23 Q. S. Chen, J. Wu, X. Y. Ou, B. L. Huang, J. Almutlaq, A. A. Zhumekenov, X. W. Guan, S. Y. Han, L. L. Liang, Z. G. Yi, J. Li, X. J. Xie, Y. Wang, Y. Li, D. Y. Fan, D. B. L. Teh, A. H. All, O. F. Mohammed, O. M. Bakr, T. Wu, M. Bettinelli, H. H. Yang, W. Huang and X. G. Liu, All-Inorganic Perovskite Nanocrystal Scintillators, *Nature*, 2018, **561**, 88–93.

24 X. J. Gu, W. C. Xiang, Q. W. Tian and S. Z. Liu, Rational Surface-Defect Control *via* Designed Passivation for High-Efficiency Inorganic Perovskite Solar Cells, *Angew. Chem., Int. Ed.*, 2021, **60**, 23164.

25 P. F. Gong, F. Liang, L. Kang, X. G. Chen, J. G. Qin, Y. C. Wu and Z. S. Lin, Recent Advances and Future Perspectives on Infrared Nonlinear Optical Metal Halides, *Coord. Chem. Rev.*, 2019, **380**, 83–102.

26 S. P. Guo, Y. Chi and H. G. Xue, $SnI_4(S_8)_2$: A Novel Adduct-Type Infrared Second-Order Nonlinear Optical Crystal, *Angew. Chem., Int. Ed.*, 2018, **57**, 11540–11543.

27 X. H. Li, Z. H. Shi, M. Yang, W. L. Liu and S. P. Guo, $Sn_7Br_{10}S_2$: The First Ternary Halogen-Rich Chalcohalide Exhibiting a Chiral Structure and Pronounced Nonlinear Optical Properties, *Angew. Chem., Int. Ed.*, 2022, **61**, e202115871.

28 R. L. Tang, W. Xu, X. Lian, Y. Q. Wei, Y. L. Lv, W. L. Liu and S. P. Guo, Na_2CeF_6: A Highly Laser Damage-Tolerant Double

Perovskite Type Ce(IV) Fluoride Exhibiting Strong Second-Harmonic Generation Effect, *Small*, 2023, 2308348.

29 W. F. Zhou and S. P. Guo, Rational Design of Novel Promising Infrared Nonlinear Optical Materials: Structural Chemistry and Balanced Performances, *Acc. Chem. Res.*, 2024, **57**, 648–660.

30 D. N. Ingebrigtson and A. L. Smith, Infrared Analysis of Solids by Potassium Bromide Pellet Technique, *Anal. Chem.*, 1954, **26**, 1765–1768.

31 D. Hahn, Calcium Fluoride and Barium Fluoride Crystals in Optics, *Opt. Photon.*, 2014, **9**, 45–48.

32 G. A. Jeffrey and M. Vlasse, Crystal Structures of the Red, Yellow, and Orange Forms of Mercuric Iodide, *Inorg. Chem.*, 1967, **6**, 396–399.

33 Y. Y. Dang, X. G. Meng, K. Jiang, C. Zhong, X. G. Chen and J. G. Qin, A Promising Nonlinear Optical Material in the Mid-IR Region: New Results on Synthesis, Crystal Structure and Properties of Noncentrosymmetric β-HgBrCl, *Dalton Trans.*, 2013, **42**, 9893.

34 G. Zhang, Y. J. Li, K. Jiang, H. Y. Zeng, T. Liu, X. G. Chen, J. G. Qin, Z. S. Lin, P. Z. Fu, Y. C. Wu and C. T. Chen, $Cs_2HgI_2Cl_2$: Molecular Engineering for a New Nonlinear Optical Material in the Infrared Region, *J. Am. Chem. Soc.*, 2012, **134**, 14818–14822.

35 T. Liu, J. Qin, G. Zhang, T. Zhu, F. Niu, Y. Wu and C. Chen, Mercury Bromide ($HgBr_2$): A Promising Nonlinear Optical Material in IR Region with a High Laser Damage Threshold, *Appl. Phys. Lett.*, 2008, **93**, 091102.

36 Y. X. Bi, L. Liu, Z. J. Yue, R. Z. Li, G. D. Zhang and X. T. Tao, Single Crystal Growth and Effect of Cleavage Micro-Striations on the Crystallinity and Optical Properties of Mercurous Halide Single Crystals, *CrystEngComm*, 2023, **25**, 2647.

37 Y. H. Zhang, F. M. Li, R. Yang, Y. Yang, F. F. Zhang, Z. H. Yang and S. L. Pan, $Rb_5Ba_2(B_{10}O_{17})_2(BO_2)$: The Formation of Unusual Functional $[BO_2]^-$ in Borates with Deep-Ultraviolet Transmission Window, *Sci. China: Chem.*, 2022, **65**, 719–725.

38 C.-M. Huang, M. Mutailipu, F. F. Zhang, K. J. Griffith, C. Hu, Z. H. Yang, J. M. Griffin, K. R. Poeppelmeier and S. L. Pan, Expanding the Chemistry of Borates with Functional $[BO_2]^-$ Anions, *Nat. Commun.*, 2021, **12**, 2597.

39 Y. Huang, Y. Zhang, D. D. Chu, Z. H. Yang, G. M. Li and S. L. Pan, HgB_2S_4: A d^{10} Metal Thioborate with Giant Birefringence and Wide Band Gap, *Chem. Mater.*, 2023, **35**, 4556–4563.

40 M. Yan, W. D. Yao, W. Liu, R. L. Tang and S. P. Guo, Helical $\{[HgS]\}_n$ Chain-Induced Balanced Nonlinear-Optical Performance for Trigonal Mercury Sulfide, *Inorg. Chem.*, 2021, **60**, 16917–16921.

41 E. Dyakonov, D. Porokhovnichenko, J. Ryu and V. Balakshy, Implementation of the Wide-Angle Acousto-Optical Interaction Geometry in a Mercury Bromide Single Crystal, *Appl. Opt.*, 2021, **60**, 2348–2353.

42 Y. X. Han, C. L. Hu and J. G. Mao, $Ca_2Ln(BS_3)(SiS_4)$ (Ln = La, Ce, and Gd): Mixed Metal Thioborate-Thiosilicates as Well-Performed Infrared Nonlinear Optical Materials, *Small*, 2023, 2305828.

43 Y. X. Han, C. L. Hu, Z. Fang, Q. Q. Chen, B. X. Li, Y. Lin and J. G. Mao, $LaBS_3$ Revisited: A Promising Mid-Infrared Nonlinear Optical Material, *J. Mater. Chem. C*, 2022, **10**, 12556–12559.

44 H. Li, G. M. Li, K. Wu, B. B. Zhang, Z. H. Yang and S. L. Pan, BaB_2S_4: An Efficient and Air-Stable Thioborate as Infrared Nonlinear Optical Material with High Laser Damage Threshold, *Chem. Mater.*, 2018, **30**, 7428–7432.

45 V. I. Pakhomov, A. V. Goryunov, I. N. Ivanova-Korfini, A. A. Boguslavskii and R. S. Lotfullin, Refinement of $HgBr_2$ Structure, *Russ. J. Inorg. Chem.*, 1990, **35**, 1407–1409.

46 Y. H. Yun, W. L. Xie, Z. H. Yang, G. M. Li and S. L. Pan, Na^+/Ag^+ Substitution Induced Birefringence Enhancement from $AgGaS_2$ to $NaGaS_2$, *J. Alloys Compd.*, 2022, **896**, 163093.

47 J. Tauc, R. Grigorovici and A. Vancu, Optical Properties and Electronic Structure of Amorphous Germanium, *Phys. Status Solidi B*, 1966, **15**, 627–637.

48 D. N. Nikogosyan, *Nonlinear optical crystals: a complete survey*, 1st edn, New York, Springer, 2005.

49 V. Kumar, K. L. A. Khan, G. Singh, T. P. Sharma and M. Hussain, ZnSe Sintered Films: Growth and Characterization, *Appl. Surf. Sci.*, 2007, **253**, 3543–3546.

50 J. Cheng, D. B. Fan, H. Wang, B. W. Liu, Y. C. Zhang and H. Yan, Chemical Bath Deposition of Crystalline ZnS Thin Films, *Semicond. Sci. Technol.*, 2003, **18**, 676.

51 A. Giordana, E. Priola, S. Pantaleone, L. Andreo, L. Mortati, P. Benzi, L. Operti and E. Diana, HgBrI: A Possible Tecton for NLO Molecular Materials, *Dalton Trans.*, 2022, **51**, 5296–5308.

52 J. Y. Guo, A. Tudi, S. J. Han, Z. H. Yang and S. L. Pan, α-SnF2: A UV Birefringent Material with Large Birefringence and Easy Crystal Growth, *Angew. Chem., Int. Ed.*, 2021, **60**, 3540–3544.

53 J. H. Wu, C. L. Hu, T. K. Jiang, J. G. Mao and F. Kong, Highly Birefringent d^0 Transition Metal Fluoroantimonite in the Mid Infrared Band: Order–Disorder Regulation by Cationic Size, *J. Am. Chem. Soc.*, 2023, **145**, 24416–24424.

54 M. Debenham, Refractive Indices of Zinc Sulfide in the 0.405–13 μm Wavelength Range, *Appl. Opt.*, 1984, **23**, 2238–2239.

55 T. M. Bieniewski and S. J. Czyzak, Refractive Indexes of Single Hexagonal ZnS and CdS Crystals, *J. Opt. Soc. Am.*, 1963, **53**, 496–497.

56 M. P. Lisitsa, L. F. Gudymenko, V. N. Malinko and S. F. Terekhova, Dispersion of the Refractive Indices and Birefringence of CdS_xSe_{1-x} Single Crystals, *Phys. Status Solidi B*, 1969, **31**, 389–399.

57 J. P. Perdew and M. Levy, Physical Content of the Exact Kohn-Sham Orbital Energies: Band Gaps and Derivative Discontinuities, *Phys. Rev. Lett.*, 1983, **51**, 1884.

58 S. S. Sahoo, V. K. Sharma, M. K. Gupta, R. Mittal and V. Kanchana, High Thermopower and Birefringence in Layered Mercury-Based Halides, *Mater. Today Commun.*, 2022, **32**, 102824.